Fully unconstrained approach to noncollinear magnetism: Application to small Fe clusters

Fully Unconstrained Approach to Noncollinear Magnetism: Application to Small Fe Clusters

Tatsuki Oda,[1,2] Alfredo Pasquarello,[1,3] and Roberto Car[1,3]

[1]*Institut Romand de Recherche Numérique en Physique des Matériaux (IRRMA), Ecublens, CH-1015 Lausanne, Switzerland*
[2]*Department of Computational Science, Faculty of Science, Kanazawa University, Kanazawa 920-11, Japan*
[3]*Department of Condensed Matter Physics, University of Geneva, CH-1211 Geneva, Switzerland*

We develop a plane-wave pseudopotential scheme for noncollinear magnetic structures, based on a generalized local spin-density theory in which the direction of the magnetization is a continuous variable of position. We allow the atomic and magnetic structures to relax simultaneously and self-consistently. Application to small Fe clusters yields noncollinear magnetic structures for Fe_3 and Fe_5. The components of the magnetization density vary smoothly with position. The spin direction undergoes sizable changes only in the regions of small charge and spin density between the atoms and is generally uniform in the magnetic regions of the atoms. [S0031-9007(98)05870-0]

PACS numbers: 75.10.$-$b, 71.15.Pd, 71.24.$+$q, 75.50.Bb

Most local spin-density calculations assumed so far complete spin alignment throughout the system, resulting in collinear magnetic structures. This approach is suitable for describing ferromagnetic or antiferromagnetic order, usually encountered in crystals. There are, however, cases where noncollinear spin arrangements may occur, such as, e.g., in the γ phase of Fe which exhibits a spin-spiral structure [1,2]. More generally, noncollinear configurations occur more easily in magnetic systems in a low symmetry or in a disordered state [3,4]. Furthermore, noncollinearity is crucial for dealing with magnetic excitations, such as spin waves, or to treat magnetism at finite temperature [5–7].

A number of generalized spin-density calculations allowing for noncollinear structures have been performed [2,5,6–12]. All of these calculations adopted the atomic sphere approximation for the crystal potential and assumed a uniform spin direction within each atomic sphere. Although the latter approximation seems well justified from a physical point of view, the actual spatial variation of spin directions as it would result from a fully unconstrained calculation is not known. In addition, the atomic sphere approximation is not reliable for atomic relaxations and, as a consequence, its application is restricted to cases in which the atomic geometry is *a priori* known.

To address the above issues, we adopt a scheme based on pseudopotentials and plane waves in which both the direction and the magnitude of the magnetization are fully unconstrained as a function of position. This approach combines noncollinear local spin-density calculations with the *ab initio* molecular dynamics method [13], which deals efficiently with the simultaneous relaxation of electronic and ionic degrees of freedom. We apply our scheme to small Fe clusters and find that some geometrical structures are characterized by noncollinear spin arrangements, which appear to be favored by an increase of the atomic spin moments. In particular, the ground state of Fe_5 is found to be noncollinear. The noncollinear structures that we find allow us to study how the spins change their orientation as a function of position and to check the validity of the common assumption of uniform spin direction within the atomic regions.

In generalized local spin-density theory [14], the wave functions are described by two-component spinors $\Psi(\mathbf{r}) \equiv (\psi_1(\mathbf{r}), \psi_2(\mathbf{r}))$, where ψ_1 and ψ_2 are complex wave functions. The density matrix is defined as

$$\rho_{\alpha\beta}(\mathbf{r}) = \sum_i f_i \psi_{\alpha i}(\mathbf{r}) \psi_{\beta i}^*(\mathbf{r}), \tag{1}$$

where α and β are spin indices and f_i is the occupation number of the ith single-particle state. In terms of the unit matrix σ_0 and of the Pauli spin matrices σ_k ($k = x, y, z$), the density matrix reads $\rho(\mathbf{r}) = \frac{1}{2} n(\mathbf{r})\sigma_0 + \frac{1}{2} \sum_k m_k(\mathbf{r})\sigma_k$, where $n(\mathbf{r})$ is the charge density and $m_k(\mathbf{r})$ is the Cartesian components of the spin density vector $\mathbf{m}(\mathbf{r})$. Note that in this scheme the individual eigenstates can have different spin quantization directions. Furthermore, the spin quantization axis of each state can vary with position.

Following the *ab initio* molecular dynamics scheme [13], we optimize simultaneously the electronic wave functions $\{\Psi_i\}$ and the atomic positions $\{\mathbf{R}_I\}$ by minimizing the total energy, which is defined for noncollinear spin structures as in Refs. [9,14]. Within our noncollinear scheme the ground-state spin moment corresponding to a given atomic structure is found automatically as a result of the minimization process. We adopt the ultrasoft pseudopotential scheme [15], which has already been used successfully to describe large d-electron systems [16]. The equations of motion for Ψ_i and R_I are solved numerically with the same procedures used in collinear cases [16]. We compute the exchange-correlation energy $E_{\text{xc}}[n(\mathbf{r}), |\mathbf{m}(\mathbf{r})|]$ with the formula given by Perdew and Zunger [17].

We demonstrate our scheme by computing structural and magnetic properties of Fe_n ($n \leq 5$) clusters. These systems have been studied extensively in the past, not only for their intrinsic interest [18–22] but also because they can be taken as simple models of the bulk [23].

TABLE I.   Bond lengths b (a.u.) and binding energies E_B (eV/atom) of magnetic Fe clusters, compared with other collinear calculations. F and AF indicate collinear ferromagnetic and antiferromagnetic structures.

Cluster				b	E_B	Figure
Fe$_2$	$D_{\infty h}$	collinear (F)	present	3.70	2.06	
			Ref. [20]	3.74	2.03	
			Ref. [21]	3.70	2.19	
			Ref. [27]	3.68	2.00	
Fe$_3$	C_{3v}	collinear (F)	present	3.99	2.64	
			Ref. [20]	3.86	2.60	
			Ref. [21]	3.97	2.75	
	$D_{\infty h}$	noncollinear	present	3.72	2.17	1(a)
	$D_{\infty h}$	collinear (AF)	present	3.66	2.15	1(b)
	$D_{\infty h}$	collinear (F)	present	3.55	1.80	
			Ref. [20]	3.63	1.79	
			Ref. [21]	3.54	2.03	
Fe$_4$	D_{2d}	collinear (F)	present	4.11,4.28	3.13	
	T_d	collinaer (F)	present	4.22	3.12	
			Ref. [20]	4.25	3.07	
			Ref. [21]	4.20	3.27	
Fe$_5$	D_{3h}	noncollinear	present	4.26,4.43	3.46	1(c)
	D_{3h}	collinear (F)	present	4.20,4.48	3.45	1(d)
			Ref. [21]	4.18,4.46	3.59	

Only collinear spin structures were considered in these studies. However, the existence of a spin-spiral phase in fcc Fe is an indication that noncollinear magnetic structures may be important in iron systems [2]. Thus small iron clusters which have less symmetry constraints than the bulk are likely candidates for the occurrence of noncollinear structures.

Our Fe pseudopotential is devised to include the semicore $3s$ and $3p$ states into the valence. In this way, the overlap of these states with the other valence states is correctly accounted for [22]. In our scheme, the inclusion of semicore states is not too costly because it does not lead to an increase of the plane-wave cutoff. Ultrasoft pseudopotentials are essentially as accurate as all-electron calculations, as shown recently for structural and vibrational properties of d-electron metals [24].

We adopt periodic boundary conditions and describe the clusters with a simple cubic unit cell having a lattice constant of 20 a.u., which is sufficient for the interactions between the periodic images to become negligible [25]. The spinor wave functions are expanded into a set of plane waves with a cutoff energy of 24 Ry. In the ultrasoft pseudopotential scheme the density matrix has a hard augmented component, for which we use a cutoff energy of 250 Ry, as described in Ref. [16]. The geometry optimizations are initiated from atomic configurations taken either from Ref. [21] or from Ref. [22]. We compute the binding energies of the clusters by taking as a reference the isolated spherical magnetic atoms with a total magnetic moment $M = 4\mu_B$. We estimate the magnetic moment of each atom in the clusters by integrating the magnetic density within spheres of radius 1.7 a.u. centered on the

atoms. These spheres do not overlap and contain about 90% of the magnetic density [26].

Our results for several optimized cluster geometries are summarized in Tables I and II. Overall, in the collinear case, our structures and binding energies agree well with previous all-electron calculations, as can be seen in Table I [28]. The only small difference with previous calculations is in the structure of Fe$_4$ with magnetic moment $M = 12\mu_B$, which was found in Refs. [20,21] to have a perfectly tetrahedral geometry. We find instead that the lowest energy structure is a distorted tetrahedron with D_{2d} symmetry, which has two short (4.11 a.u.) and four long (4.28 a.u.) bond lengths. We recover a regular tetrahedron (T_d) by using fractional occupation numbers ($f_i = 1/3$) for the triply degenerate highest occupied molecular orbital. The corresponding bond length is 4.22 a.u. and the binding energy is only 0.01 eV/atom higher than that of the ground state, which can be considered as a Jahn-Teller distortion of the regular tetrahedron [29].

We find noncollinear spin arrangements for Fe$_3$ and Fe$_5$ clusters of symmetry $D_{\infty h}$ [linear chain, Fig. 1(a)] and D_{3h} [trigonal bipyramid, Fig. 1(c)], respectively. We notice that in both cases the loss of collinearity results in a coplanar magnetic structure. The noncollinear Fe$_5$ structure corresponds to the ground state, whereas the noncollinear Fe$_3$ structure is metastable. In the latter case, the ground state is collinear and has the structure of an equilateral triangle (C_{3v} symmetry). In both non-collinear cases, we find a collinear cluster of the same symmetry [Figs. 1(b) and 1(d), respectively] at a slightly higher energy (0.01−0.02 eV/atom). The noncollinear structures have larger atomic magnetic moments and, on

TABLE II. Total M and atomic M_{at} magnetic moments (in units of μ_B) of Fe clusters. F and AF are as in Table I. For noncollinear structures, the vector components of the atomic moments are also given.

	Cluster		M (M_{at})	Figure
Fe	spherical	collinear (F)	4.00 (3.29)	
Fe$_2$	$D_{\infty h}$	collinear (F)	6.00 (2.67)	
Fe$_3$	C_{3v}	collinear (F)	8.00 (2.44)	
	$D_{\infty h}$	noncollinear	2.04 (2.89,1.27)	1(a)
		Fe (edge)	(±2.88, 0.00, 0.29)	
		Fe (central)	(0.00,0.00,1.27)	
	$D_{\infty h}$	collinear (AF)	0.00, (2.88,0.00)	1(b)
	$D_{\infty h}$	collinear (F)	6.00 (1.84,1.04)	
Fe$_4$	D_{2d}	collinear (F)	12.00 (2.62)	
	T_d	collinaer (F)	12.00 (2.61)	
Fe$_5$	D_{3h}	noncollinear	14.57 (2.71,2.72)	1(c)
		Fe (apical)	(±1.34, 0.00, 2.35))	
		Fe (basal)	(0.00,0.00,2.72)	
	D_{3h}	collinear (F)	14.00 (2.55,2.58)	1(d)

average, slightly elongated bond lengths, compared with their collinear counterparts. This suggests that non-collinearity is favored by the magnetic energy associated with larger magnetic moments. This energy competes with the chemical bonding energy which is reduced for stretched bonds. A correlation between bond distances and spin multiplicity was already observed in the case of magnetic dimers [30].

The noncollinear magnetic structure of Fe$_3$ resembles that of its collinear antiferromagnetic counterpart. With respect to the latter, the central atom acquires a finite moment and the moments of the edge atoms are tilted by 10°, yielding a total moment of $2.04\mu_B$. Note that the direction of the total magnetic moment is arbitrary since we do not include spin-orbit effects. In the case of Fe$_5$ the total magnetic moment has a magnitude of $14.57\mu_B$ and is parallel to the moments of the atoms in the basal plane. The moments of the two apical atoms are tilted
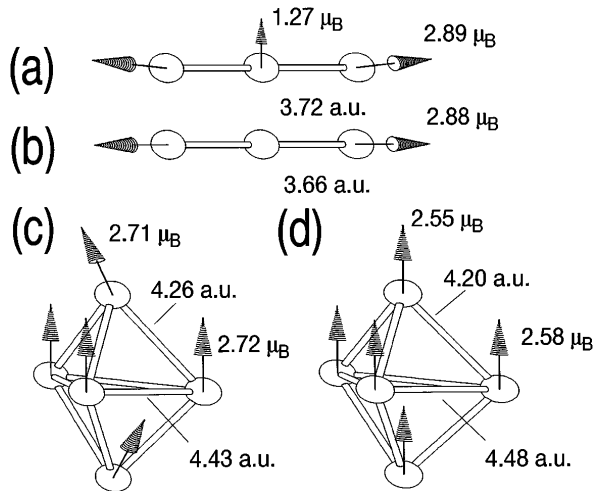

FIG. 1. Atomic and magnetic structures of noncollinear (a) Fe$_3$ and (c) Fe$_5$. The corresponding collinear structures are given in (b) and (d).

in opposite directions by approximately 30° (Table II) with respect to the moments of the basal atoms. The noncollinear spin configurations that we obtain in Fe$_3$ and Fe$_5$ suggest a ferromagnetic interaction between nearest neighbors and an antiferromagnetic interaction between next-nearest neighbors. Interestingly, similar features are also observed in calculations of the exchange parameters of bulk fcc Fe [8,10].

In Figs. 2(a) and 2(b) we report the spatial variation of the magnitude of the magnetization density together with the charge density along some special directions in Fe$_3$ and Fe$_5$ clusters, respectively. The spatial localization of the magnetization density reflects that of the $3d$ states. On the nuclei, our calculated magnetization density is not accurate because of the pseudopotential approximation. However, this has a negligible effect on our calculated properties since the integrated magnetization over a small volume close to the nuclei is well reproduced [31]. Next, we define a Cartesian reference frame in which the z axis is parallel to the direction of the total magnetization and the x-z plane is the plane in which the direction of the magnetization density varies. The x and z components of the magnetization density are reported in Figs. 2(c) and 2(d). These components vary going from one atom to the other, indicating a change of direction of the magnetization. Overall, the components are as smooth as the magnitude of the magnetization. In order to better characterize the variation of the spin direction we plot in Figs. 2(e) and 2(f) the polar angle θ formed by the magnetization density and the z axis ($-180° \leq \theta < 180°$). The spin direction is remarkably uniform within the regions surrounding the atoms that carry a large magnetic moment, such as the
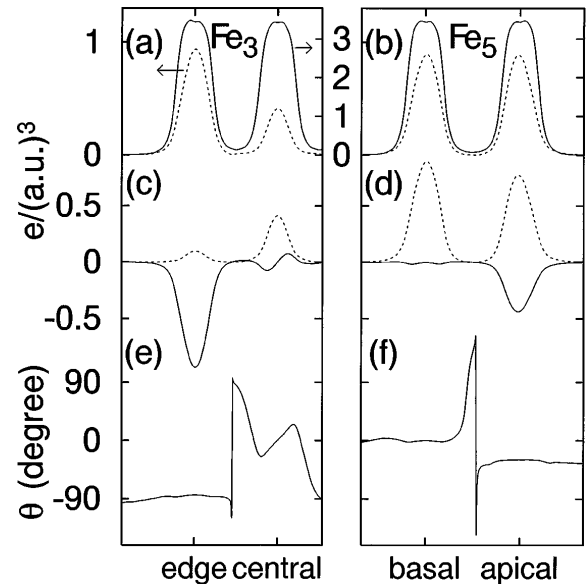

FIG. 2. Noncollinear magnetization density along the symmetry axis of Fe$_3$ and along a line connecting a basal and an apical atom in Fe$_5$. Charge (solid line) and modulus of the magnetization density (dashed line) for (a) Fe$_3$ and (b) Fe$_5$, corresponding x (solid line) and z (dashed line) components in (c) and (d), and the corresponding polar angle θ in (e) and (f).

edge atoms in the trimer and all of the atoms in the pentamer. Typically the dispersion of the spin direction is of about 1° for these atoms. Around the central atom of the trimer, which carries a relatively small magnetic moment, the spin direction makes a small oscillation. This appears to be induced by a ferromagnetic coupling with the two edge atoms which have spins pointing in almost opposite directions. The occurrence of a small magnetic moment on one atom is peculiar and is likely related to the fact that this is not the ground-state configuration of the trimer. As shown in Figs. 2(e) and 2(f), the spin direction changes abruptly in the interatomic regions, where the magnetization density is essentially zero and the charge density is very small. The change in spin direction shows a large fluctuation related to a spin flip in the interatomic region. This appears to be a general feature that occurs both in collinear and in noncollinear cases.

We note that all of the collinear structures reported in Table I are local minima. This implies, in particular, that there are barriers separating the noncollinear and their corresponding collinear structures in Fig. 1. This is inconsistent with a simple picture based on a classical Heisenberg Hamiltonian and is likely related to the increase of atomic moments when going from the collinear structures to their noncollinear counterparts.

So far, in all studies of noncollinear magnetism, a coarse graining procedure was adopted which associates a single spin direction to each atomic sphere. Our finding that the spin direction is uniform within a given sphere supports this approximation. Interestingly, although the magnetization density has a uniform direction within each atomic sphere, the spin quantization axes of single eigenstates inside each sphere vary both from state to state and with position.

In order to study spin fluctuations at finite temperature it is important to treat noncollinear magnetic structures [5–7]. This requires a description not only of the magnetic density within the atomic spheres but also of the rapid variation of spin direction in the interatomic region, which gives an important contribution to the kinetic energy [32].

In conclusion, we have presented the first application of a fully unconstrained scheme for noncollinear magnetism. The self-consistent treatment of orbital, magnetic, and atomic degrees of freedom makes our scheme a promising tool for investigations of magnetic systems from first principles.

[1] Y. Tsunoda, J. Phys. Condens. Matter **1**, 10 427 (1988).

[2] O. N. Mryasov, A. I. Liechtenstein, L. M. Sandratskii, and V. A. Gubanov, J. Phys. Condens. Matter **3**, 7683 (1991).

[3] R. Lorenz, J. Hafner, S. S. Jaswal, and D. J. Sellmyer, Phys. Rev. Lett. **74**, 3688 (1995).

[4] M. Liebs, K. Hummler, and M. Fähnle, Phys. Rev. B **51**, 8664 (1995).

[5] L. M. Sandratskii and P. G. Guletskii, J. Magn. Magn. Mater. **79**, 306 (1989).

[6] V. P. Antropov, M. I. Katsnelson, M. van Schilfgaarde, and B. N. Harmon, Phys. Rev. Lett. **75**, 729 (1995); V. P. Antropov, M. I. Katsnelson, B. N. Harmon, M. van Schilfgaarde, and D. Kusnezov, Phys. Rev. B **54**, 1019 (1996).

[7] M. Uhl and J. Kübler, Phys. Rev. Lett. **77**, 334 (1996).

[8] A. I. Liechtenstein, M. I. Katsnelson, V. P. Antropov, and V. A. Gubanov, J. Magn. Magn. Mater. **67**, 65 (1987).

[9] J. Kübler, K. Höck, J. Sticht, and A. R. Williams, J. Phys. F **18**, 469 (1988).

[10] T. Oguchi, K. Terakura, and N. Hamada, J. Phys. F **13**, 145 (1983).

[11] M. Uhl, L. M. Sandratskii, and J. Kübler, Phys. Rev. B **50**, 291 (1994).

[12] L. M. Sandratskii and J. Kübler, Phys. Rev. Lett. **76**, 4963 (1996).

[13] R. Car and M. Parrinello, Phys. Rev. Lett. **55**, 2471 (1985).

[14] U. von Barth and L. Hedin, J. Phys. C **5**, 1629 (1972).

[15] D. Vanderbilt, Phys. Rev. B **41**, 7892 (1990).

[16] A. Pasquarello, K. Laasonen, R. Car, C. Lee, and D. Vanderbilt, Phys. Rev. Lett. **69**, 1982 (1992); K. Laasonen, A. Pasquarello, R. Car, C. Lee, and D. Vanderbilt, Phys. Rev. B **47**, 10 142 (1993).

[17] J. P. Perdew and A. Zunger, Phys. Rev. B **23**, 5048 (1981).

[18] H. Tatewaki, M. Mutsumi, M. Tomonari, and T. Nakamura, J. Chem. Phys. **88**, 6419 (1988).

[19] S. Dhar and N. R. Kestner, Phys. Rev. A **38**, 1111 (1988).

[20] J. L. Chen, C. S. Wang, K. A. Jackson, and M. R. Pederson, Phys. Rev. B **44**, 6558 (1991).

[21] M. Castro and D. R. Salahub, Phys. Rev. B **49**, 11 842 (1994).

[22] P. Ballone and R. O. Jones, Chem. Phys. Lett. **233**, 632 (1995).

[23] C. Y. Yang, K. H. Johnson, D. R. Salahub, J. Kaspar, and R. P. Messmer, Phys. Rev. B **24**, 5673 (1981).

[24] A. D. Corso, A. Pasquarello, and A. Baldereschi, Phys. Rev. B **56**, R11 369 (1997).

[25] G. Makov and M. C. Payne, Phys. Rev. B **51**, 4014 (1995); M. R. Jarvis, I. D. White, R. W. Godby, and M. C. Payne, Phys. Rev. B (to be published).

[26] The magnetic density is slightly less localized for an isolated atom (see Table II).

[27] P. E. Blöchl, Phys. Rev. B **50**, 17 953 (1994).

[28] For the dimer we find a vibrational frequency of 453 cm^{-1}, close to other calculations [19–21,27].

[29] Starting the geometry optimization from the C_{2v} configuration proposed in Ref. [22], we also converge to the D_{2d} ground state.

[30] J. Harris and R. O. Jones, J. Chem. Phys. **70**, 830 (1979).

[31] The radius of this volume is determined by the pseudoization of the augmented charge [16] and it is approximately equal to 1 a.u. in the present calculation.

[32] V. Korenman, J. L. Murray, and R. E. Prange, Phys. Rev. B **16**, 4032 (1977).